Journal of Cranio-Maxillo-Facial Surgery 47 (2019) 1378–1386

Contents lists available at ScienceDirect

Journal of Cranio-Maxillo-Facial Surgery

journal homepage: www.jcmfs.com

Evaluation of a novel algorithm for automating virtual surgical planning in mandibular reconstruction using fibula flaps

Ali Modabber*, Alexandra Rauen, Nassim Ayoub, Stephan Christian Möhlhenrich, Florian Peters, Kristian Kniha, Frank Hölzle, Stefan Raith

Department of Oral, Maxillofacial and Facial Plastic Surgery, RWTH Aachen University Hospital, Aachen, Germany

ARTICLE INFO

Article history:
Paper received 22 February 2019
Accepted 19 June 2019
Available online 25 June 2019

Keywords:
Mandibular reconstruction
Fibula flap
Automated algorithm
Virtual surgical planning
Computer-assisted surgery

ABSTRACT

Virtual surgical planning plays an increasingly important role in jaw reconstruction. The aim of the present study was the evaluation of the clinical applicability of a novel algorithm for automating virtual mandibular reconstruction using fibula flaps.

The software uses Computed-Tomography of the facial skeleton and the lower leg of 63 subjects, implemented in Python programming language. The developed algorithm is based on individual bone curvatures of the mandible and fibula. Ten different defects were generated for each mandible by virtually defined cutting planes. Three experienced surgeons reviewed all reconstruction proposals generated by the algorithm according to a visual analogue scale. The possible correlation between the ratings and the prioritization of the algorithm and the calculation time for the reconstructions were analyzed.

Spearman analysis showed a strong correlation −0.613 ($p < 0.001$) between the deviation of the reconstruction result from the target line and the average assessment of the surgeons as well as a moderate correlation −0.448 ($p = 0.013$) between surgeons' assessments and the prioritization by the algorithm. The calculation time for twenty reconstructions per defect took between 4.99 s and 483.5 s depending on defect size and location.

The evaluated algorithm automatically creates valid reconstruction results with acceptable computation time, which have received a high level of confirmation from experienced surgeons.

1. Introduction

The maxillofacial area uniquely combines important functional and aesthetic aspects within a close topography. The mandible plays a central role in this context. In addition, it allows for mastication and swallowing and it enables correct articulation. At the same time, the lower jaw defines the profile of a face and determines the outer appearance of the lower third of the face (Wallace et al., 2010). The loss of mandibular continuity leads to functional as well as aesthetic restrictions, which makes reconstructive procedures inevitable. In contrast to reconstruction plates, microvascular transplants can achieve better results and make this particular procedure “state of the art” (Levine et al., 2012).

In the case of extensive, mixed oromandibular defects, the microsurgical fibula flap is considered state of the art among the free vascularized flaps (Disa et al., 1999; Klesper et al., 2000; Graham et al., 2003; Hölzle et al., 2011).

The fibula flap was first described by Taylor in 1975 (Taylor et al., 1975). In 1983, Chen and Yan reported for the first time an osteocutaneous fibula graft, thus enabling not only the supply of the bony component, but also the coverage of extensive soft tissue defects (Chen and Yan, 1983). In 1989, Hidalgo described the first application of a microvascular fibula flap in the reconstruction of a mandible was described. Through osteotomies within the straight fibula, the curvature of the mandible could be reproduced (Hidalgo, 1989). However, the investigators reported, concerning vitality of a microvascular fibula flap, that the length of the fibular segments should not be less than 20 mm (Bähr, 1998).

The microvascular fibular transplant is characterized by its extensive bony length of up to 20–30 cm (Taylor et al., 1975; Chen and Yan, 1983; Hidalgo, 1989; Cordeiro et al., 1999) and it permits

* Corresponding author. Department of Oral, Maxillofacial and Facial Plastic Surgery, RWTH Aachen University Hospital, Pauwelsstr. 30, 52074, Aachen, Germany. Fax: +49 241 8082430.
E-mail address: amodabber@ukaachen.de (A. Modabber).

https://doi.org/10.1016/j.jcms.2019.06.013
1010-5182/

reconstruction of the mandible from angle to angle (Wei et al., 1994; Anthony et al., 1995). In addition, the skin flap shows great adaptability (Wei et al., 1986, 1994) and through the septum great flexibility. Other advantages of the microvascular flap are the possibility of double barreling to gain height (Bähr et al., 1998; Wallace et al., 2010) and the possibility of a two-team approach during the surgery (Hidalgo, 1989; Flemming et al., 1990; Wallace et al., 2010).

The conventional process of intraoperative flap adaptation and shaping to the given defect is a very time-intensive and lengthy endeavor. By using computer-assisted surgery (CAS), the transplant planning can be performed preoperatively. In this way, it is possible to foresee intraoperative difficulties (Antony et al., 2011). Moreover, the ischemic period of the transplant can be reduced intraoperatively (Roser et al., 2010) and alternative concepts could be developed (Antony et al., 2011). The operation time represents one of the most important cost factors. An optimization of the process in the form of preoperative, virtual surgical planning can thus directly reduce costs through reduced surgical time, which can compensate the additional costs incurred by CAS (Hanasono and Skoracki, 2010; Modabber et al., 2012a).

Thus, by the use of CAS, mandibular reconstruction can be simplified and a patient-specific bestreconstruction result can be achieved (Modabber et al., 2012b).

The transmission of virtual reconstruction planning into the operating room can be carried out by so-called “cutting guides”, which are produced according to the CAD-CAM method, typically with modern additive manufacturing techniques (Klimek et al., 1993; Ewers et al., 2005; Juergens et al., 2009; Leiggener et al., 2009; Roser et al., 2010; Lethaus et al., 2012; Levine et al., 2012; Modabber et al., 2012a,b).

Roser et al. demonstrated high accuracy in the agreement between the virtual reconstruction planning and the real reconstruction result and confirmed the positive effect of virtual planning in the context of mandibular reconstruction (Roser et al., 2010). Alternative transmission mechanisms are stereotactic systems, however, requiring further development. In the age of rapidly-developing technology, further optimization of given standards is constantly necessary.

Raith et al. described an algorithm for computer-aided planning of mandible reconstructions that provides a semi-automated workflow relying on individual mandibular defects and corresponding fibulas. His approach is based on the principle of reducing the complex, three-dimensional structures to a curve in order to simplify the task (Raith et al., 2018). The goal in the future is to get an acceptable reconstruction suggestion from workflow, after uploading 3D files of the mandible and fibula and setting individual parameters with one mouse click, so that cutting guides for this proposal could be directly printed for clinical use.

Therefore, the aim of this study was to evaluate the reconstruction proposals of CAS by automating virtual reconstruction planning using the described algorithm in order to pave the way for routine use in clinical mandibular reconstruction cases.

2. Materials and methods

2.1. Automated algorithm for reconstruction planning

For the automated creation of reconstruction proposals, a custom, in-house developed software package was used (Raith et al., 2018). This software has been implemented in the Python programming language (version 3.5) and takes advantage of the user interface of the open software tool Blender (version 2.77, Blender Foundation, Amsterdam, Netherlands), i. e. a free GPL-licensed 3D graphics software that allows, among other things, modeling, texturing, rendering, and animation of three-dimensional objects. Because the software's source code is freely available, it offers full flexibility to adjust specific components of the software to special needs, such as the demands of surgical planning (The Blender Foundation: www.blender.org/about).

The tailored software tool that was used in the present study needed specific individual geometrical input, such as the geometry of the reconstruction target shape (i. e. the defect) and residual bony parts (i. e. in the present study the mandible) and geometry of the donor bone (i. e. the fibula in the present study). Both structures need to be imported as segmented surface data, originating from volumetric imaging, such as computed tomography (CT), CT-Angiography (CTA) or cone beam computed tomography (CBCT).

A mandatory step guiding the automatic reconstruction is the manual definition of two specific curves on the virtual bone surfaces. One of these curves is drawn at the reconstruction site (Fig. 1) that marks the external contour of the desired shapes to be reconstructed, and it can be individually adjusted according to the aesthetic or later prosthetic requirements. Because it is desired to restore the outer contour of the face for aesthetic rehabilitation, it is usually desired to follow this outer (i. e. caudolateral) contour of the resected part of the mandible. For further clinical prerequisites, such as rehabilitation of masticatory function, the contour of the curve may be adjusted arbitrarily by the user in three-dimensional space. The second curve that needs to be defined manually for subsequent automated reconstruction planning needs to be placed at the donor site, following the curvature of the fibula. Margins for protection spaces can be defined to prevent extensive bone harvest, because clinical experience shows the stability of the ankle joint would be compromised when too much fibular bone is harvested (Sonmez et al., 2013; Ghassemi et al., 2016) and proximal injury of the common peroneal nerve can occur.

Aside from this manual definition of the two anatomical curves, all other parameters can be chosen by the software automatically, though there potentially would be a graphical front end to allow specific user input at that stage also. The number of segments was chosen as fixed values per defect type, selected according to experience from preliminary studies (Table 1).

The length of these segments was automatically chosen by the computer according to a random process. It is important to note that not all segment lengths can be individually specified, because the length of the last segment is calculated to close the remaining gap in the direction of the residual mandible part. Thus, its length is a result of the previous length distributions and the individual curvature of the target curve.

The actual calculation of the reconstruction planning is executed within a fully-automated procedure. Aside from the visualization of the reconstruction planning, the integrated distance between the target curve and the transplant curve is calculated as a scalar numeric value. All resulting data can be stored in a custom file format and exported as images, geometrical data (e. g. in.stl file format) and numeric values as Microsoft Excel data sheets.

The algorithm that was used in this study is described more precisely in detail in a previous publication of our group (Raith et al., 2018). There, the interested reader can find additional information on the implementation background of the method and the use of the software interface.

2.2. Geometry data, segmentation and creation of virtual defects

All geometrical data used in the present study were generated from routinely performed diagnostic CT of both the head and neck area and the lower leg of the same subjects ($n = 63$). Both sets of image data permit acquisition of bone geometries of the mandible and the fibula as the desired donor bone. The relevant bony structures were found to be intact by visual inspection and also did

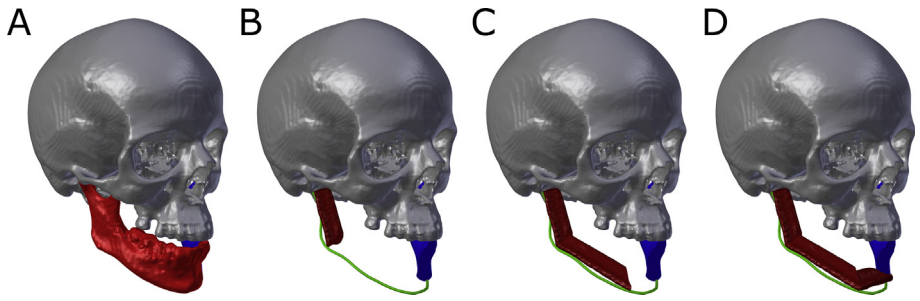

Fig. 1. Example of an automated virtual reconstruction (HC defect) A) Segmented mandible surface with missing and residual parts displayed in red and blue, respectively; B) First segment of a fibula at reconstruction site positioned at the ascending ramus (caudo-lateral contour of the reconstruction site displayed in green); C) Additional display of second segment at the mandibular corpus; D) Additional display of third segment at the mental region.

Table 1
Number of segments per defect (based on the mandibular classification of Jewer (Jewer et al., 1989)).

Defect	C	C+	H	H+	HC	HCL	L	L+	LC	LCL
Number of segments	1	2	3	2	3	4	2	1	2	3

not show any signs of malformations, which would be an exclusion criterion. All CT scans were obtained with a 128-row multi-slice CT scanner, Somatom Definition Flash (Siemens, Erlangen, Germany). Acquisition of scans for the head and neck was done in 0.5 mm slice thickness, and for the fibula, in 1 mm slice thickness. Segmentation of the data was performed with the commercial software package, ProPlan CMF version 1.4 (Materialise Inc., Leuven, Belgium), and the resultant triangulated surface data of both bony regions were stored in.stl file format. Both fibulas were segmented in the study and workflow allows the choice between the left and right fibula for reconstruction. However, the left fibula of each subject was considered for virtual grafting.

2.3. Target geometry curves and protected spaces

Both target curve and transplant curve were drawn once on each mandible and each corresponding fibula, respectively, as described above. The target curves that correspond to the individual defects were generated by automatically by truncation of the whole mandibular curve while using the same cutting planes that were used to divide the residual and the missing mandible parts in the creation of the virtual defects.

In the present study, protection margins at the fibula were set to 70 mm from both the ankle and knee (Sonmez et al., 2013; Ghassemi et al., 2016). We implemented this constraint to only allow clinically feasible transplant sections to be selected, because a literature survey showed common recommendations for protection margins between 6 and 8 cm (Wolff et al., 1996, 2011; Shpitzer et al., 1997; Blake et al., 2008; Collin et al., 2008; Chaine et al., 2009). The program additionally has an implementation of a threshold value for minimal segment length, because short segments tend to show clinical problems as blood vessel supply is more problematic in short transplant sections. In the scope of this study we used the default threshold value of 20 mm (Bähr, 1998). In the present study, we chose the relative position on the harvesting site to be always 70 mm distance from the ankle.

2.4. Virtual defects

For the evaluation of the algorithm, ten different defects were generated by virtually defined cutting planes. According to classification of Jewer et al., (1989), these defects are named C, C+, H, H+, HC, HCL, L, L+, LC, and LCL (Fig. 2). The defects with a "+" are modifications of the corresponding original classification with smaller or lager defects. Cases where the whole mandible is missing (HH according to Jewer et al.) were initially included in the study, but in general, the available portion of the fibula was found to be insufficient to reconstruct the whole missing mandible shape. Thus, only limited data would have been available for statistical evaluation. Hence, it was decided to completely remove this defect from the study design within the scope of this work.

2.5. Study design

2.5.1. Automatic preparation of reconstruction designs

All reconstruction designs were generated automatically. Within this process, the program chose the free parameters, i. e. segment lengths, by applying randomly chosen factors between 1 and 6 that were multiplied with the given constraint for minimal segment lengths that was set to 20 mm. In the present study, this value was chosen because short segments tend to show clinical problems as blood vessel supply is more problematic in short transplant sections (Bähr, 1998). An exception was made for the relatively large defects HC and LC, where we chose a minimal length of 35 mm because short segments proved to be less well-suited for reconstruction planning in the approach chosen in the current study. As a pilot study demonstrated, in these two defects a very large proportion of invalid designs would have been generated otherwise, increasing calculation times unnecessarily.

It is important to note that the minimal segment length to classify a design as valid was not only calculated along the fibula curve, but also inside, toward the oral cavity. We reached this decision because it might occur otherwise that the minimal length criterion is fulfilled along the outside, but due to the wedge-shaped osteotomies, inside the segments might become too short (Fig. 3). A further clinical constraint was that the angle between adjacent segments was not allowed to be less than 90° (Fig. 3).

For each of the ten defects in each subject ($n = 63$), we sought to achieve 20 different valid reconstruction proposals with random parameters. However, because all the clinical constraints had to be fulfilled, not all combinations of parameters yielded valid designs. Thus, in some cases, it was necessary to calculate more than twenty parameter combinations to reach twenty valid designs. In some cases, e.g. especially for large defects, the available part of the fibula would not be sufficient to bridge the gap, thus, there were only a few parameter combinations that allowed valid designs. In worst-case scenarios, no valid designs could be achieved at all. Thus, a stop criterion for the calculation of the twenty valid designs was implemented that was set to sixty minutes per single defect.

Following the actual calculation of each reconstruction proposal, five sample images were generated from standardized views: (1)

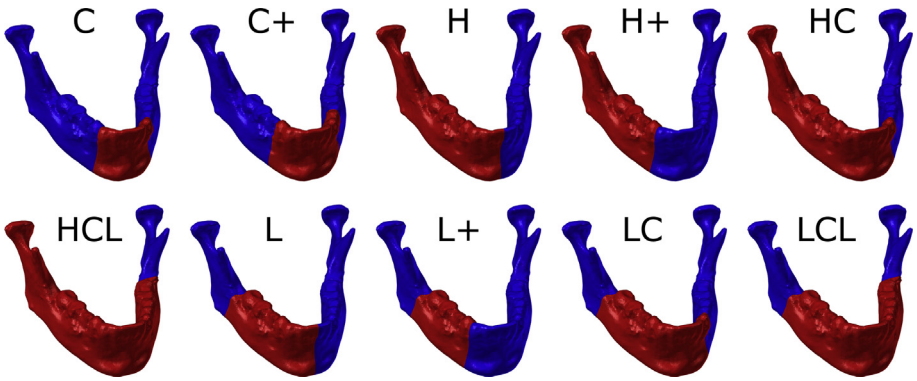

Fig. 2. Example defects created by cutting the mandible to match defects according to the definition of Jewer et al., (1989). Residual parts defects are displayed in blue and red, respectively. In total, ten different defect types were selected and virtually generated for the present study: C, C+, H, H+, HC, HCL, L, L+, LC, and LCL.

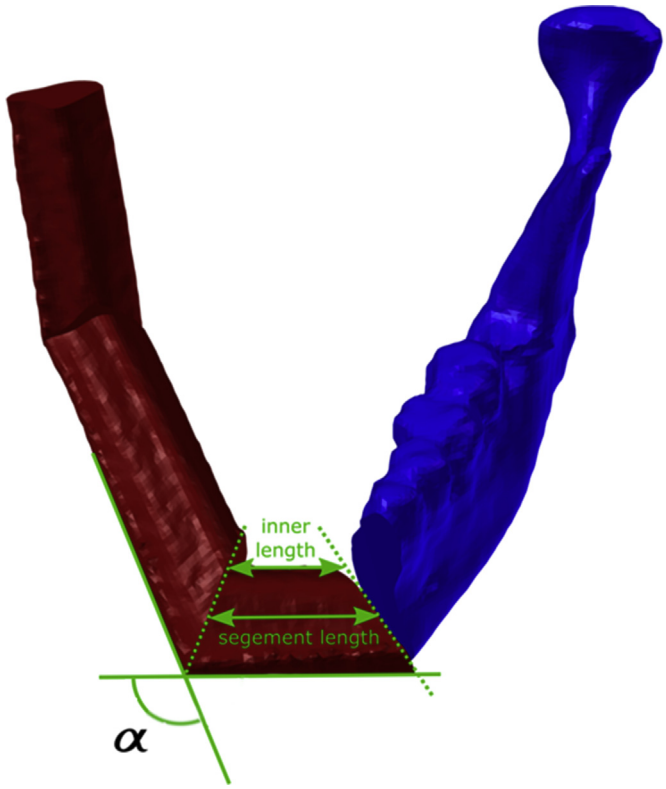

Fig. 3. Visualization of the principle of measuring the inner length by consideration of the angulated cuts (dotted line). These lengths are used as references for the comparison to the minimal length threshold. Relative angle between the segments are measured in 3D (displayed as α).

lateral view from right, (2) frontal view, (3) lateral view from left, (4) bottom view and (5) top view (the latter with hidden maxilla and skull). Additionally, the geometrical accordance between each proposed reconstruction and the known missing shape was quantified by calculation of an integrated three-dimensional deviation, as previously published [27] and stored in a separate file with custom format. Subsequently, all twenty reconstruction proposals were ordered according to the calculated value of geometrical accordance. Then, three samples were considered to be presented for the final visual evaluations. Those were the best design, the second best and the tenth best (i. e. an average design, as it is the tenth out of twenty) (Fig. 4).

Three independent and experienced surgeons (later called examiners) reviewed all reconstruction proposals that were generated by the automated algorithm. To standardize that procedure, five automatically generated sample described above were displayed on a computer screen in a schematic order (Fig. 5). At the time of image review, all examiners were blinded to the numerical rating, i. e. whether the currently-investigated reconstruction was the best, second or tenth in the order of all twenty reconstructions per case. The examiners then had the possibility to rate the reconstruction design according to a visual analogue scale (VAS) that was also displayed on the computer screen next to the sample images (Fig. 5). The VAS displayed labeled marks at a step size of 25% and unlabeled marks at a step size of 5% to permit better orientation for the examiners and thus better reproducibility. With mouse interaction the rating mark (displayed in red) could be placed along the VAS according to the judgment of the examiners and subsequently the resulting data of the VAS could be exported and stored in Microsoft Excel file format. Like the reconstruction software, the evaluation tool had been implemented in the Python programming language (version 3.5) and the user interface was provided by Blender (version 2.77, Blender Foundation, Amsterdam, Netherlands).

2.6. Statistical analysis

The data generated by the examiners' assessment were investigated for the following questions. All analyses were tested previously for normal distribution, and the threshold value for the significance was defined as p-value < 0.05. In order to investigate whether the examiners differed significantly in their assessment of the reconstruction proposals, a one-way ANOVA variance analysis was used. A possible correlation between the examiners' ratings and the prioritization of the program (into first, second and tenth best results of the reconstruction proposals) was checked by Spearman correlation. A correlation between the assessment of the three examiners and the deviation between the target curve and the transplant curve, which is given as a numerical value and which is the basis for the prioritization of the reconstruction proposals by the program, also was tested by means of Spearman correlation. For the calculation time and for the deviation between the target and transplant curve, the arithmetic mean including the standard deviation was calculated. We performed the statistical analysis on that data with the software GraphPad Prism 6® (GraphPad Software, Inc., USA).

3. Results

For nine of the ten types of defects, all cases could be calculated. The only exception was the large HCL defect that failed to deliver

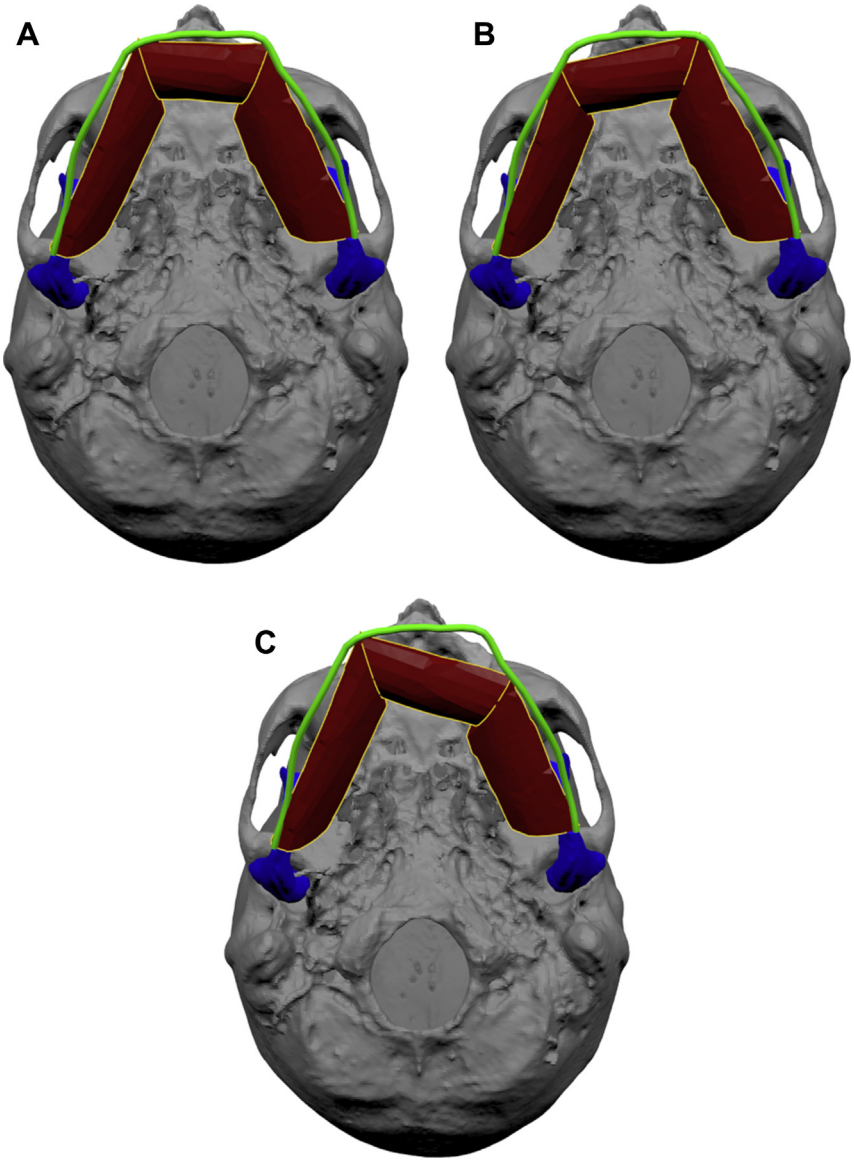

Fig. 4. Examples of reconstruction results of an LCL defect from the five standardized perspectives, A) first best reconstruction proposal; B) second best reconstruction proposal; C) tenth best reconstruction proposal.

enough valid reconstruction designs within the predefined scope of sixty minutes. For this defect, in 41 out of 63 cases (65.1%), we achieved the required number of twenty valid designs. Thus, only these were used in the subsequent statistical evaluations.

Hence, in total 12,160 reconstruction designs were calculated for consideration. Out of those data, 1,824 reconstruction designs were chosen to be presented to the three examiners, thus yielding 5,472 evaluations using the screen display and the rating with VAS on a scale of 0–100 %. A value of 0 % represents the situation in which the surgeon disagrees with the proposal. A value of 100 % indicates that the surgeon would actually translate the proposed reconstruction 1 to 1 into reality. The analysis shows that examiner 1 and examiner 2 ($p = 0.008$) and examiner 2 and 3 ($p = 0.0056$) differ significantly, but no significant difference exists in the assessment of reconstructions between examiner 1 and 3 ($p = 0.9447$) (Fig. 6). Spearman correlation gives a correlation coefficient of -0.448 ($p = 0.013$) between the three surgeons' assessments and the prioritization of the reconstruction results by the program. The bar graph (Fig. 7) shows that the tenth best reconstruction proposals received, on average, always less than or nearly equal scores compared to the best and second best proposals. Except for the defect classes HC and HCL, the ratings of the other defects by default showed high confirmation. Applying the Spearman test, we checked for a possible correlation between the deviation of the reconstruction result from the target line and the average assessment of the surgeons. The correlation coefficient was -0.613 ($p = 0.0003$). Fig. 8 visualizes the scatter plot. An approximate negative linear relationship between the deviation and the mean score becomes apparent.

In 63 patient cases, the program generated twenty reconstruction proposals for each defect class. The bar chart visualizes the time required to generate twenty valid reconstruction proposals. The minimum generation time was 4.99 s for the C defect (as this one and L+ were the ones with only one segment); the most time the program needed to generate twenty reconstruction proposals was for the HCL defect. At this point, the mean was 483.5 s (Fig. 9). Fig. 10 visualizes the average deviation of the first, second and tenth best reconstruction proposals from the target

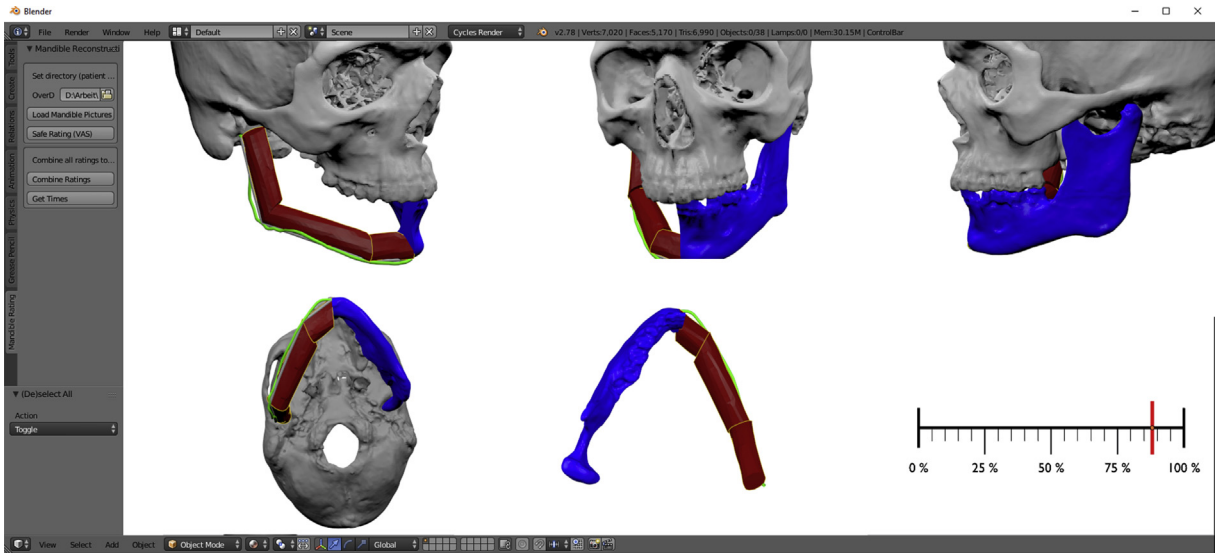

Fig. 5. Screenshot of the evaluation tool. Five different views of the reconstruction proposal are displayed. Additionally, the VAS (bottom right), that allows adjustment of the rating with mouse interactions is displayed. All numerical rating data is stored automatically in Excel file format.

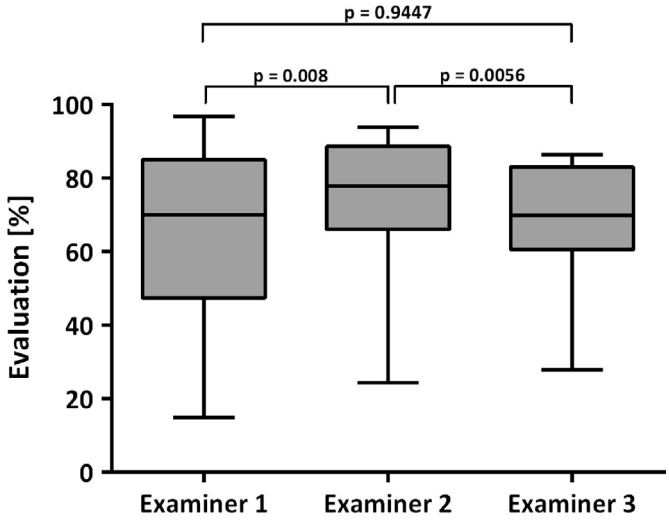

Fig. 6. Rating of the examiner 1, 2 and 3.

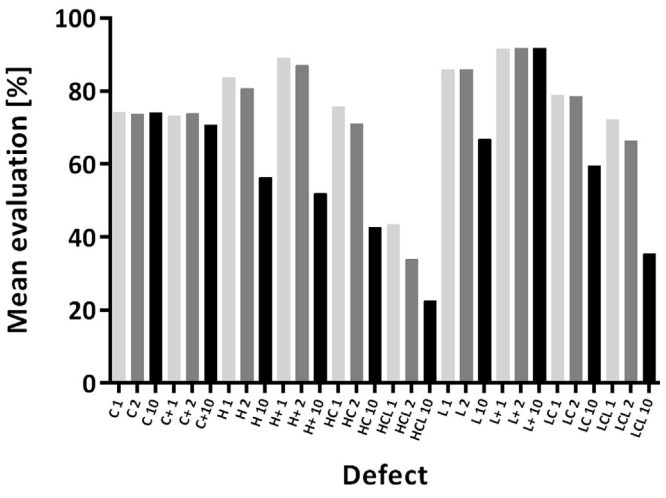

Fig. 7. Mean evaluations of all examiners per defect class.

line per defect class. Large standard deviations in defect classes C and L+ are noticeable.

4. Discussion

CAS offers the opportunity to meet the high requirements of reconstructive surgery. In the future, this kind of automated procedure should allow the surgeon to find the best solution for the patient, even if the surgeon is not experienced in planning. By means of CAS for planning, it should be possible for the surgeon to create the best surgical plan in a short amount of time.

To create surgical plans for bony reconstructions, the defects have to be classified. In the literature, different classifications for defects of the lower jaw are prescribed (David et al., 1988; Jewer et al., 1989; Urken et al., 1991; Boyd et al., 1993; Iizuka et al., 2005; Baumann et al., 2011). The most common classification is the HCL classification developed by Jewer. In our study, the additional C+, H+ and L+ defects were added to the HCL classification. This was necessary to refine the classification of defects. With respect to testing the clinical usage of our program, the classification more closely approximated reality with continuous transitions between the different defect sizes. For the evaluation of the reconstructions, three samples were considered. In addition to the best and second outcome, we chose the tenth reconstruction proposal to sufficiently detect possible differences.

The surgeon's primary purpose is to reconstruct the curvature of the mandible (Nakao et al., 2017). Our custom software tries to reach the highest possible level of congruence between the fibular curve and the mandibular curve that marks the defect of the lower jaw. Deficiencies of the curve are allowed, but excrescences over the determined structure are not implemented. This simplification allows reduction of the complex three-dimensional structure of the lower jaw to a two-dimensional curve representing the determined structure of the transplant. The reduction to two-dimensional structures simplifies the workflow so that there is no need for time-consuming training for the end users (Raith et al., 2018). Another advantage of the method presented in this paper is the acceptable time for generating a reconstruction. At present, the algorithm presented here needs 483.5 s to create twenty proposals

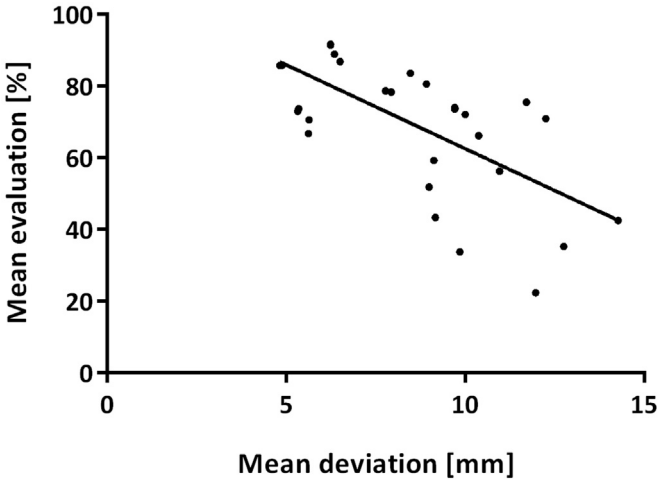

Fig. 8. Scatter plot of mean deviation and mean score of all examiners with linear regression line.

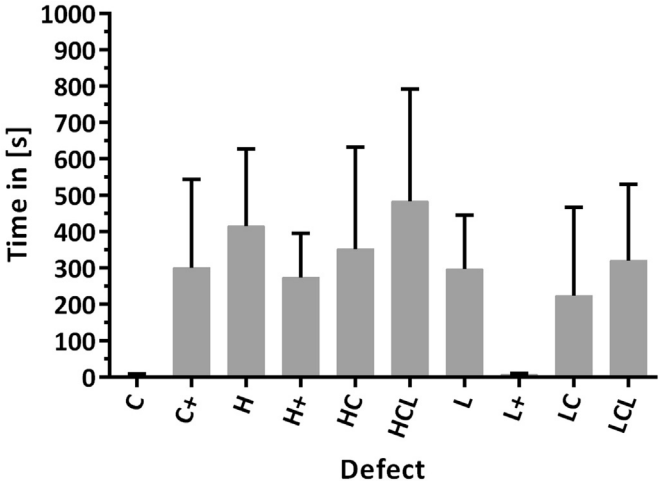

Fig. 9. Mean calculation time for 20 reconstruction proposals per defect class.

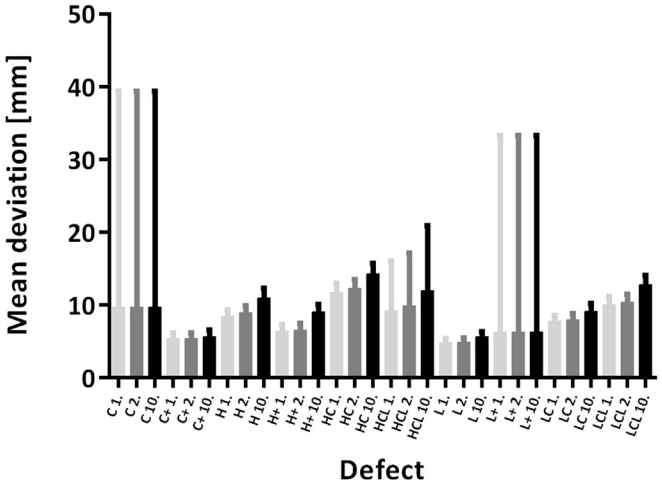

Fig. 10. Mean deviation per defect.

for an HCL defect. The HCL defect is the most complicated one evaluated here and requires the most computing time, with an average of 24.2 s per defect as determined on a standard personal computer. In comparison, the program of Nakao et al. (2017) needs a computing time of 33.3 ± 3.8 s for a two-segment reconstruction and 43.5 ± 5.5 s for a three-segment reconstruction. However, Nakao et al. used superior hardware for their measurement of computation time. If the algorithm developed by Nakao et al. would be executed on a standard personal computer, a significantly longer computing time could be expected.

The HCL defect was the singular situation for which valid reconstruction proposals could not be generated for all patient cases. The reason for this problem could be found in the fact that this is the longest defect. Moreover, in some subjects, that available portion of the fibula is not sufficient to restore this large missing part of the mandible.

In contrast to the fairly simple method used in the present study, Nakao et al. described a much more complicated way of finding the best transplant. In their paper, the whole three-dimensional surface of the mandible is taken into account (Nakao et al., 2013, 2015, 2017). Supposedly, their software required special training and computational expertise that makes routine usage of this approach in the usual clinical setting not feasible. However, Nakao et al. developed an objective function that not only considers the deviations of the planned reconstruction from the original form of the lower jaw, but also takes into account symmetry parameters, which is of significant importance and might ameliorate our method in further stages of development. Concerning the large variability of defects of the lower jaw and the limited possibility of contouring fibular transplants, a compromise between deviation and symmetry needs to be found. In the study by Nakao et al., the surgeon and the algorithm preferred the same solution for reconstruction only when both parameters—symmetry and deviation—were used for calculation (Nakao et al., 2017).

In our study, significant differences could be found between the three different examiners who assessed the proposed reconstruction of the mandible. These differences reflected inter-individual differences between the three examiners. These significant differences could be expected to occur during clinical practice. Even if the examiners differ significantly, the correlation between these examiners' ratings and the program's prioritization exhibits a significant correlation (coefficient of −0.448) with a moderate negative relationship. Therefore, the best proposed solution by the program is usually associated with the best assessment of the surgeon. Also, the parameter “deviation” (between the result and the target line) is a sufficient parameter for computing the reconstructions. The correlation coefficient of −0.613 shows a strong negative correlation between the surgeons' assessment and the deviation between the result and the target line.

During this study, the fibular reconstruction program was constrained to perform an osteotomy in the graft to cover a C defect. Additionally, the program does not permit fitting the fibula segment in front of the residual mandibular body. Thus, there was a relatively large deviation from the target line in these cases. The situation is similar in defect class L+. There is no osteotomy planned in the graft. The large standard deviation of the defect classes C and L+, shown in Fig. 10, could be a result of the restrictions given to the program.

Comparing individual defects, the HCL defect is noticeable. The mean of the first HCL reconstructions in relation to the surgical assessment is significantly lower in comparison to all other first proposed reconstruction proposals (mean of surgical assessment of the HCL defect: 43.38 %; Fig. 7). Additionally, the calculation of the HCL reconstructions required considerably more time (mean of calculation time of the HCL defect: 483.5 s; Fig. 9).

The problem with the ideal reconstruction of this defect is that the program does not allow crossing the target line and thus the last, mental segment often falls below the minimum segment

length of 20 mm. Thus, an asymmetrical reconstruction resulted, which did not find a high rating among the examiners. By accounting for symmetrical aspects and the exceeding of the target line in selected cases, the reconstructions could be further refined, while increasing computing time as an accompanying drawback.

5. Conclusion

In summary, the present workflow based on the novel algorithm automatically generates mandibular reconstructions using microvascular fibula flaps with moderate computation time. It creates valid reconstruction results, which have received a high level of confirmation from experienced maxillofacial surgeons despite inter-individual differences. The algorithm shows a moderate correlation between surgeons' evaluation and program prioritization of the reconstructions, as well as a strong correlation between the deviation of the reconstructions and the surgical assessment.

The algorithm is a revolutionary, basic approach in preoperative, computer-aided surgery planning, which should be further enhanced and developed in the future, thus expanding it into a multivariate function that integrates further clinical aspects, such as double barreling, the position of the skin flap, appropriate connection vessels and corresponding requirements for subsequent prosthetic planning that should be integrated into the workflow. The aim is a completely comprehensive automated, mandibular reconstruction which takes all clinical aspects into account.

Conflicts of interest

The authors declare that they have no conflict of interest.

Acknowledgements

We are grateful to Ms Lindsey Zeichner for language editing of our manuscript. Furthermore, we want to thank Medartis (Basel, Switzerland) for financial support of the present study.

This article is based on the thesis of Alexandra Rauen, which has not yet been submitted at the time of publication.

References

Anthony JP, Rawnsley JD, Benhaim P, Ritter EF, Sadowsky SH, Singer MI: Donor leg morbidity and function after fibula free flap mandible reconstruction. Plast Reconstr Surg 96: 146–152, 1995

Antony AK, Chen WF, Kolokythas A, Weimer KA, Cohen MN: Use of virtual surgery and stereolithography-guided osteotomy for mandibular reconstruction with the free fibula. Plast Reconstr Surg 128: 1080–1084, 2011

Bähr W: Blood supply of small fibula segments: an experimental study on human cadavers. J Craniomaxillofac Surg 26: 148–152, 1998

Bähr W, Stoll P, Wächter R: Use of the "double barrel" free vascularized fibula in mandibular reconstruction. J Oral Maxillofac Surg 56: 38–44, 1998

Baumann DP, Yu P, Hanasono MM, Skoracki RJ: Free flap reconstruction of osteoradionecrosis of the mandible: a 10-year review and defect classification. Head Neck 33: 800–807, 2011

Blake F, Heiland M, Schmelzle R, Harms J, Werle H, Pohlenz P, et al: The medial approach to the fibula: a feasible alternative. J Oral Maxillofac Surg 66: 319–323, 2008

Boyd JB, Gullane PJ, Rotstein LE, Brown DH, Irish JC: Classification of mandibular defects. Plast Reconstr Surg 92: 1266–1275, 1993

Chaine A, Pitak-Arnnop P, Hivelin M, Dhanuthai K, Bertrand JC, Bertolus C: Postoperative complications of fibular free flaps in mandibular reconstruction: an analysis of 25 consecutive cases. Oral Surg Oral Med Oral Pathol Oral Radiol Endod 108: 488–495, 2009

Chen ZW, Yan W: The study and clinical application of the osteocutaneous flap of fibula. Microsurgery 4: 11–16, 1983

Collin T, Sugden P, Ahmed O, Ragbir M: Technical considerations of fibular osteocutaneous flap dissection. J Plast Reconstr Aesthet Surg 61: 1503–1506, 2008

Cordeiro PG, Disa JJ, Hidalgo DA, Hu QY: Reconstruction of the mandible with osseous free flaps: a 10-year experience with 150 consecutive patients. Plast Reconstr Surg 104: 1314–1320, 1999

David DJ, Tan E, Katsaros J, Sheen R: Mandibular reconstruction with vascularized iliac crest: a 10-year experience. Plast Reconstr Surg 82: 792–803, 1988

Disa JJ, Hidalgo DA, Cordeiro PG, Winters RM, Thaler H: Evaluation of bone height in osseous free flap mandible reconstruction: an indirect measure of bone mass. Plast Reconstr Surg 103: 1371–1377, 1999

Ewers R, Schicho K, Undt G, Wanschitz F, Truppe M, Seemann R, et al: Basic research and 12 years of clinical experience in computer-assisted navigation technology: a review. Int J Oral Maxillofac Surg 34: 1–8, 2005

Flemming AF, Brough MD, Evans ND, Grant HR, Harris M, James DR, et al: Mandibular reconstruction using vascularised fibula. Br J Plast Surg 43: 403–409, 1990

Ghassemi A, Schreiber L, Prescher A, Modabber A, Nanhekhan L: Regions of ilium and fibula providing clinically usable bone for mandible reconstruction: "A different approach to bone comparison". Clin Anat 29: 773–778, 2016

Graham RG, Swan MC, Hudson DA, van Zyl JE: The fibula free flap: advantages of the muscle sparing technique. Br J Plast Surg 56: 388–394, 2003

Hanasono MM, Skoracki R: Improving the speed and accuracy of mandibular reconstruction using preoperative virtual PLanning and rapid prototype modeling. Plast Reconstr Surg 125: 80, 2010

Hidalgo DA: Fibula free flap: a new method of mandible reconstruction. Plast Reconstr Surg 84: 71–79, 1989

Hölzle F, Ristow O, Rau A, Mucke T, Loeffelbein DJ, Mitchell DA, et al: Evaluation of the vessels of the lower leg before microsurgical fibular transfer. Part I: anatomical variations in the arteries of the lower leg. Br J Oral Maxillofac Surg 49: 270–274, 2011

Iizuka T, Hafliger J, Seto I, Rahal A, Mericske-Stern R, Smolka K: Oral rehabilitation after mandibular reconstruction using an osteocutaneous fibula free flap with endosseous implants. Factors affecting the functional outcome in patients with oral cancer. Clin Oral Implant Res 16: 69–79, 2005

Jewer DD, Boyd JB, Manktelow RT, Zuker RM, Rosen IB, Gullane PJ, et al: Orofacial and mandibular reconstruction with the iliac crest free flap: a review of 60 cases and a new method of classification. Plast Reconstr Surg 84: 391–403, 1989 Discussion 404–395

Juergens P, Krol Z, Zeilhofer HF, Beinemann J, Schicho K, Ewers R, et al: Computer simulation and rapid prototyping for the reconstruction of the mandible. J Oral Maxillofac Surg 67: 2167–2170, 2009

Klesper B, Wahn J, Koebke J: Comparisons of bone volumes and densities relating to osseointegrated implants in microvascularly reconstructed mandibles: a study of cadaveric radius and fibula bones. J Craniomaxillofac Surg 28: 110–115, 2000

Klimek L, Klein HM, Schneider W, Mosges R, Schmelzer B, Voy ED: Stereolithographic modelling for reconstructive head surgery. Acta Otorhinolaryngol Belg 47: 329–334, 1993

Leiggener C, Messo E, Thor A, Zeilhofer HF, Hirsch JM: A selective laser sintering guide for transferring a virtual plan to real time surgery in composite mandibular reconstruction with free fibula osseous flaps. Int J Oral Maxillofac Surg 38: 187–192, 2009

Lethaus B, Poort L, Bockmann R, Smeets R, Tolba R, Kessler P: Additive manufacturing for microvascular reconstruction of the mandible in 20 patients. J Craniomaxillofac Surg 40: 43–46, 2012

Levine JP, Patel A, Saadeh PB, Hirsch DL: Computer-aided design and manufacturing in craniomaxillofacial surgery: the new state of the art. J Craniofac Surg 23: 288–293, 2012

Modabber A, Legros C, Rana M, Gerressen M, Riediger D, Ghassemi A: Evaluation of computer-assisted jaw reconstruction with free vascularized fibular flap compared to conventional surgery: a clinical pilot study. Int J Med Robot 8: 215–220, 2012a

Modabber A, Gerressen M, Stiller MB, Noroozi N, Fuglein A, Hölzle F, et al: Computer-assisted mandibular reconstruction with vascularized iliac crest bone graft. Aesth Plast Surg 36: 653–659, 2012b

Nakao M, Aso S, Imai Y, Ueda N, Hatanaka T, Shiba M, et al: Automated planning with multivariate shape descriptors for fibular transfer in mandibular reconstruction. IEEE Trans Biomed Eng 64: 1772–1785, 2017

Nakao M, Hosokawa M, Imai Y, Ueda N, Hatanaka T, Kirita T, et al: Volumetric fibular transfer planning with shape-based indicators in mandibular reconstruction. IEEE J Biomed Health Inform 19: 581–589, 2015

Nakao M, Hosokawa M, Imai Y, Ueda N, Hatanaka T, Minato K, et al: Volumetric surgical planning system for fibular transfer in mandibular reconstruction. Conf Proc IEEE Eng Med Biol Soc 2013: 3367–3370, 2013

Raith S, Rauen A, Mohlhenrich SC, Ayoub N, Peters F, Steiner T, et al: Introduction of an algorithm for planning of autologous fibular transfer in mandibular reconstruction based on individual bone curvatures. Int J Med Robot 14, 2018

Roser SM, Ramachandra S, Blair H, Grist W, Carlson GW, Christensen AM, et al: The accuracy of virtual surgical planning in free fibula mandibular reconstruction: comparison of planned and final results. J Oral Maxillofac Surg 68: 2824–2832, 2010

Shpitzer T, Neligan P, Boyd B, Gullane P, Gur E, Freeman J: Leg morbidity and function following fibular free flap harvest. Ann Plast Surg 38: 460–464, 1997

Sonmez TT, Prescher A, Salama A, Kanatas A, Zor F, Mitchell D, et al: Comparative clinicoanatomical study of ilium and fibula as two commonly used bony donor sites for maxillofacial reconstruction. Br J Oral Maxillofac Surg 51: 736–741, 2013

Taylor GI, Miller GD, Ham FJ: The free vascularized bone graft. A clinical extension of microvascular techniques. Plast Reconstr Surg 55: 533–544, 1975

The Blender Foundation, www.blender.org/about

Urken ML, Weinberg H, Vickery C, Buchbinder D, Lawson W, Biller HF: Oromandibular reconstruction using microvascular composite free flaps. Report of 71 cases and a new classification scheme for bony, soft-tissue, and neurologic defects. Arch Otolaryngol Head Neck Surg 117: 733–744, 1991

Wallace CG, Chang YM, Tsai CY, Wei FC: Harnessing the potential of the free fibula osteoseptocutaneous flap in mandible reconstruction. Plast Reconstr Surg 125: 305–314, 2010

Wei FC, Chen HC, Chuang CC, Noordhoff MS: Fibular osteoseptocutaneous flap: anatomic study and clinical application. Plast Reconstr Surg 78: 191–200, 1986

Wei FC, Seah CS, Tsai YC, Liu SJ, Tsai MS: Fibula osteoseptocutaneous flap for reconstruction of composite mandibular defects. Plast Reconstr Surg 93: 294–304, 1994 Discussion 305–296

Wolff KD, Ervens J, Herzog K, Hoffmeister B: Experience with the osteocutaneous fibula flap: an analysis of 24 consecutive reconstructions of composite mandibular defects. J Craniomaxillofac Surg 24: 330–338, 1996

Wolff KD, Hölzle F, Kolk A, Hohlweg-Majert B, Steiner T, Kesting MR: Raising the osteocutaneous fibular flap for oral reconstruction with reduced tissue alteration. J Oral Maxillofac Surg 69: e260–e267, 2011